Biochimica et Biophysica Acta 1828 (2013) 1690–1699

Contents lists available at SciVerse ScienceDirect

Biochimica et Biophysica Acta

journal homepage: www.elsevier.com/locate/bbamem

The substitution of Arg149 with Cys fixes the melibiose transporter in an inward-open conformation

Yibin Lin [a], Oliver Fuerst [a], Meritxell Granell [a], Gérard Leblanc [b], Víctor Lórenz-Fonfría [a,1], Esteve Padrós [a,*]

[a] Unitat de Biofísica, Departament de Bioquímica i de Biologia Molecular, Facultat de Medicina, and Centre d'Estudis en Biofísica, Universitat Autònoma de Barcelona, 08193 Bellaterra, Barcelona, Spain

[b] Institut de Biologie et Technologies-Saclay, Service de Bioenergétique, Biologie Structurale et Mécanismes, CEA-Saclay, F-91191 Gif sur Yvette, France

ARTICLE INFO

Article history:
Received 1 August 2012
Received in revised form 15 February 2013
Accepted 1 March 2013
Available online 15 March 2013

Keywords:
Infrared difference spectroscopy
Förster resonance energy transfer
Membrane vesicle

ABSTRACT

The melibiose transporter from *Escherichia coli* (MelB) can use the electrochemical energy of either H^+, Na^+ or Li^+ to transport the disaccharide melibiose to the cell interior. By using spectroscopic and biochemical methods, we have analyzed the role of Arg149 by mutagenesis. According to Fourier transform infrared difference and fluorescence spectroscopy studies, R149C, R149Q and R149K all bind substrates in proteoliposomes, where the protein is disposed inside-out. Analysis of right-side-out (RSO) and inside-out (ISO) membrane vesicles showed that the functionally active R149Q and R149K mutants could bind externally added fluorescent sugar analog in both types of vesicles. In contrast, the non-transporting R149C mutant does bind the fluorescent sugar analog as well as melibiose and Na^+ in ISO, but not in RSO vesicles. Therefore, the mutation of Arg149 into cysteine restrains the orientation of transporter to an inward-open conformation, with the inherent consequences of a) reducing the frequency of access of outer substrates to the binding sites, and b) impairing active transport. It is concluded that Arg149, most likely located in the inner (cytoplasmic) half of transmembrane helix 5, is critically involved in the reorientation mechanism of the substrate-binding site accessibility in MelB.

1. Introduction

Membrane transport proteins play a decisive role in the uptake and release of solute molecules by prokaryotic and eukaryotic cells, mediating numerous important physiological processes. Removal of neurotransmitters from the synaptic cleft by selective transporters, or regulation of the cell's intracellular pH and cell volume by pumps and antiporters is a relevant example [1,2]. Another important example corresponds to sugar transporters, present in most cellular membranes. The *Escherichia coli* melibiose transporter (MelB) is a member of the glycoside–pentoside–hexuronide:cation symporter family, which in turn forms part of the major facilitator superfamily. It is a secondary active transporter, coupling the uphill transport of melibiose (a disaccharide consisting of one galactose and one glucose moiety in an α(1–6) glycosidic linkage) towards the cytoplasm, to the downhill entry of H^+, Na^+ or Li^+ in a 1:1 ratio [3–5]. The transport takes place through several steps involving substrate binding, translocation and release ([4]; see Supplementary Fig. S1). As in other secondary transporters, the translocation is expected to take place by means of an alternating access mechanism, where the structurally coupled substrate-binding sites present access to the extracellular medium in the binding process, and to the cytoplasmatic medium in the release process [6]. The presence of intermediate states in the alternating access mechanism has been reported for some transporters [7,8], and it is postulated as well for MelB [9–11].

MelB is composed of 473 amino acids and, according to secondary structure predictions, biochemical analyses, and homology studies, it consists of 12 transmembrane helices organized as two bundles of 6 helices, with both the N- and C-terminal in the cytoplasmic side [12–14]. In the last years, several atomic structures of Na^+/solute transporters have been resolved [15–17]. They share several characteristics of the transport mechanism; however, some important aspects vary. The number of transmembrane helices and their organization, the stoichiometry (1, 2 or more Na^+ per solute) and/or the order of Na^+/substrate release may differ. Also important is the nature of the ligands used for Na^+ binding. As an example, the sodium galactose transporter vSGLT of *Vibrio parahaemolyticus* uses mainly carbonyl oxygens from the main chain [16], whereas MelB mainly uses oxygens from Asp side chains [18,19]. Much less is known about the nature of the amino acids governing the outward/inward facing reorientations of the substrate-binding sites, arguably the core of the translocation mechanism for any secondary transporter.

In a search for important amino acids for sugar transport in MelB, it was demonstrated the importance of Arg149, an amino acid located

Abbreviations: MelB, melibiose transporter from *Escherichia coli*; TM, transmembrane; RSO, right-side-out; ISO, inside-out; IR_{diff}, Fourier transform infrared difference; FRET, Förster resonance energy transfer; D^2G, 2′-(N-dansyl)-aminoethyl-1-thio-D-galactopyranoside; MTSET, (2-(trimethylammonium)ethyl) methane thiosulfonate; TMRM, tetramethylrhodamine-5-maleimide; $K_{0.5}$ [Na^+], constant of activation by Na^+; $K_{0.5}$ [mel], constant of the inhibition by melibiose; LacY, lactose transporter from *E. coli*

* Corresponding author. Tel.: +34 93581870; fax: +34 935811907.
E-mail address: esteve.padros@uab.cat (E. Padrós).
[1] Present address: Department of Physics, Freie Universität, 14195 Berlin, Germany.

0005-2736/$ – see front matter © 2013 Elsevier B.V. All rights reserved.
http://dx.doi.org/10.1016/j.bbamem.2013.03.003

presumably in the inner (cytoplasmic) half of TM5. The R149C mutant was found to be completely inactive for melibiose transport in *E. coli* cells and unable to bind sugars, while R149K and R149Q mutants retained some transport activity [20].

To decipher the structural and/or catalytic defect responsible for the transport inactivation in R149C, we present in this work spectroscopic and biochemical data reporting on the substrate-induced conformational changes and protein accessibility in vesicles and in proteoliposomes. Fourier transform infrared difference (IR_{diff}) spectroscopy [19,21] has been used to bring information on the global transporter structure and on the substrate-induced conformational changes triggered by the binding of Na^+ and melibiose to the Arg149 mutants. On the other hand, fluorescence spectroscopy has been used to complement this structural analysis, as well as to determine the protein orientation and the binding site accessibility in vesicles using a fluorescent probe for Cys residues and a fluorescent sugar analog [20,22,23]. We found that, while R149C cannot bind substrates added to the external medium in RSO membrane vesicles, it binds externally added substrates when reconstituted into liposomes or in inside-out (ISO) membrane vesicles. In contrast, the active mutants R149Q and R149K are able to bind substrates in both ISO and RSO vesicles, although only R149K shows a native-like substrate-binding accessibility behavior. In contrast to a previous suggestion proposing a lack of substrate binding as the inactivating defect in R149C [20], we conclude that Arg149 is critically involved in the reorientation mechanism of the substrate-binding sites of the MelB transporter.

2. Materials and methods

2.1. Materials

Tetramethylrhodamine-5-maleimide (TMRM) was obtained from Sigma-Aldrich. (2-(trimethylammonium)ethyl) methane thiosulfonate bromide was obtained from Affymetrix, Inc. Synthesis of the fluorescent sugar analog 2′-(N-dansyl)-aminoethyl-1-thio-D-galactopyranoside (D^2G) was carried out by Dr. B. Rousseau and Y. Ambroise (Institut de Biologie et Technologies-Saclay, CEA, France). *E. coli* total lipid extract for the reconstitution of proteins was from Avanti Polar Lipids, Inc. All other materials were of reagent grade and obtained from commercial sources.

2.2. MelB expression, purification, and reconstitution

MelB and the mutants were cloned, expressed and purified similarly as previously reported [5]. In short, a recombinant pK95ΔAHB plasmid with a cassette containing the melB gene encoding a permease with a 6-His-tag at its C-terminal end [5] and devoid of its four native cysteines (Cys-less MelB) [24] was used as a background for further permease engineering and as a control. The proteins were overexpressed in *E. coli* DW2-R (ΔmelB, ΔlacZY) transformed with the appropriate plasmid, grown at 30 °C in M9 medium supplemented with 0.5% glycerol, 0.2% (w/v) casaminoacids, 10 mM thiamine, and 0.1 mM ampicillin, until an OD600 of 1.6–1.8 was reached [25]. For the purification of the transporters, cells were homogenized in a medium containing 50 mM Tris–HCl (pH 8.0), 50 mM NaCl, and 5 mM 2-mercaptoethanol and disrupted using a microfluidizer (Model 110S, Microfluidics) with 3 passes at 20,000 psi. Cell debris were removed by low-speed centrifugation for 10 min. The supernatant was collected and ultracentrifuged at 310,000 *g* for 30 min. The membrane fraction was incubated with 1% (w/v) 3-(laurylamido)-N, N′-dimethylaminopropylamine oxide (LAPAO, Anatrace) for 30 min at 4 °C. Following another ultracentrifugation step at 310,000 *g* for 15 min, the supernatant was collected and loaded to a Ni^{+2}-NTA affinity resin (Sigma-Aldrich) and washed with 20 mM Tris, 100 mM NaCl, 10% glycerol, 10 mM melibiose, 10 mM imidazole, 0.1% (w/v) dodecyl-β-D-maltopyranoside (DDM, Anatrace), and 5 mM 2-mercaptoethanol at pH 8.0. The protein was eluted at pH 8.0 with 100 mM imidazole and 0.1% DDM. MelB reconstitution into liposomes of *E. coli* total lipids (protein/lipid ratio 1/2, w/w) was performed by removing the detergent with Bio-Beads SM-2 (Bio-Rad). MelB content was assayed by a Lowry procedure including 0.2% (w/v) sodium dodecyl sulfate and using bovine serum albumin as standard [26].

2.3. Preparation of membrane vesicles

RSO and ISO membrane vesicles were prepared from the same culture. RSO membrane vesicles were prepared after lysozyme–ethylenediaminetetraacetic acid treatment and RNase and osmotic lysis [5,27]. In order to remove whole cells and partially lysed forms from the membrane preparation, the RSO membrane vesicle pellet was resuspended in 100 mM KPi (pH 6.6), containing 10 mM $MgSO_4$ and 20% sucrose. The suspension was carefully layered on top of 60% sucrose (w/v) containing 100 mM KPi buffer (pH 6.6), and 10 mM $MgSO_4$ and centrifuged at 64,000 *g* overnight. The thick layer of the membrane remaining at the interface was carefully aspirated, diluted with 100 mM KPi (pH 6.6), 10 mM $MgSO_4$ and centrifuged at 146,000 *g* until clear. The purified RSO vesicles were washed several times with the same buffer, and resuspended to a protein concentration of 10–20 mg/ml in 100 mM KPi (pH 6.6), frozen in liquid nitrogen, and stored at −80 °C until use.

ISO membrane vesicles were prepared by microfluidizer pressure, which is similar to a French press. The cell debris and unbroken cell were removed by low-speed centrifugation for 30 min, and the supernatant was collected and centrifuged at 146,000 *g* for 30 min. The ISO membrane vesicles were washed 3–4 times with 100 mM KPi buffer (pH 6.6), and resuspended in the same buffer at about 10–20 mg of protein/ml, frozen in liquid nitrogen and stored at −80 °C until use.

MelB content of membrane vesicles was measured using the histidine-Tag-specific reagent His-Probe™-HRP (Thermo scientific) directed against the 6His introduced at the C-terminus of the transporter sequence, following the manufacturer's protocol. In short, membrane samples (10 μg protein) were incubated with the SDS-PAGE loading buffer containing 2% SDS for 5 min at room temperature and loaded on a 12%-SDS-PAGE gel. After electrophoresis, the proteins were transferred to nitrocellulose (NC) membranes, blocked with Tris-buffered saline containing 25 mg/ml bovine serum albumin for 1 h and washed twice with Tris-buffered saline. The NC membranes were then incubated with the His-Probe™-HRP reagent for 1 h at room temperature and washed 3 times with buffer. After this, the NC membranes were developed by incubation with the SuperSignalWorking Solution containing luminol and peroxide and quantified with the ImageJ software.

2.4. Site-directed alkylation of cysteine

Site-directed alkylation of cysteine was carried out following a protocol as described [28–30] with some modifications. TMRM was dissolved in dimethyl sulfoxide (DMSO) and the concentration determined by measuring absorbance in methanol at 541 nm (extinction coefficient, 95,000 cm^{-1} M^{-1}). RSO or ISO membrane vesicles (about 0.1 mg of total protein in 200 μL of 100 mM KPi buffer at pH 7.5) were incubated in the presence or in the absence of 0.1 mM MTSET on ice for 5 min. Reactions were stopped by adding 1.4 ml of ice-cold 100 mM KPi buffer (pH 7.5), and centrifuged. Pellets were washed 3 times with the same buffer, and resuspended in 200 μl 100 mM KPi buffer (pH 7.5). TMRM was added at final concentration of 40 μM, and incubated on ice for 30 min. Reactions were terminated at the indicated time by adding 10 mM dithiothreitol (DTT). The membranes were then incubated with 2% DDM at 4 °C for 30 min on a rotating platform. The solubilized protein was incubated with 25 μl Ni-NTA affinity resin for 1 h and centrifuged at 1000 *g* for 1 min. The pellet was washed 6 times with 100 mM KPi buffer (pH 7.5), 100 mM NaCl, 10 mM imidazole and the protein was eluted with 25 μl of the same buffer containing 300 mM imidazole. The samples were then subjected to sodium dodecyl sulfate-polyacrylamide gel electrophoresis (SDS-PAGE). The wet gels sandwiched

between glass plates were then imaged directly on an Imager VersaDoc MP 4000 System (Bio-Rad). The Cy3 laser setting (excitation at 532 nm) with a 580 nm filter (emission wavelength) was used to capture the image. The SDS-PAGE gels were then Coomassie stained and scanned. The TMRM signal and amount of protein were estimated by measuring the density of each band by using Quantity One software (Bio-Rad).

2.5. FT-IR difference spectra

The experimental setup was the same as that described in a previous study [21]. In summary, a volume of MelB containing proteoliposome suspension (~100 μg of protein) in 100 mM KCl, 20 mM MES (pH 6.6) was spread homogeneously on a germanium ATR crystal (Harrick, Ossining, NY; 50 × 10 × 2 mm, yielding 12 internal reflections at the sample side) and dried under a stream of nitrogen. The substrate-containing buffer and the reference buffer were alternatively perfused over the proteoliposome film at a rate of ~1.5 ml/min. The film was exposed to the substrate-containing buffer for 4 min and washed with the reference buffer for 10 min (or 30 min for the buffer containing 50 mM melibiose). For each cycle, 1000 scans at a resolution of 4 cm^{-1} were recorded and a minimum of 25 spectra were taken and averaged in order to increase the signal-to-noise ratio (i.e., a total of ≥25,000 scans for every difference spectrum). Spectra were recorded with an FTS6000 Bio-Rad spectrometer equipped with a Mercury–Cadmium–Telluride detector. Data corrections for the difference spectra were carried out following a protocol developed previously [21]. Deconvolution by the maximum entropy method was applied to the difference spectra as previously described to resolve overlapped bands [31].

2.6. Quantitative comparison of intensity and similarity of FTIR difference spectra

Quantitative comparison of intensity and similarity of IR_{diff} spectra were performed as described [19]. In brief, all the difference spectra presented were normalized for the amount of protein contributing to the IR signal in the 1700–1500 cm^{-1} interval, which includes the protein conformation-sensitive amide I and amide II bands from the peptide bond. Quantitative comparison of two normalized difference spectra (an input and a reference spectrum) was performed by a linear regression in the 1710–1500 cm^{-1} interval on the first derivative of the difference spectra and in the 1700–1500 cm^{-1} on the second derivative of the absorbance spectra. The correlation analysis provides two relevant parameters: a) the correlation coefficient (R^2), which shows the spectral similarity of the input with respect to the reference spectrum in response to the added substrate; and b) the slope, which quantifies the relative intensity of common features in the input with respect to the reference spectrum arising in response to the effect of substrates.

2.7. Fluorescence spectra

Fluorescence measurements were performed at 20 °C with a UV–visible QuantaMaster™ spectrofluorometer and processed with the Felix 32 software (Photon Technology International). Trp fluorescence spectra were obtained by setting the excitation wavelength at 290 nm (half-bandwidth of 5 nm) and collecting the emission spectrum in 100 mM KPi and pH 7.0. Na^+-dependent FRET signals (λ_{ex}, 290 nm; half-bandwidth, 5 nm) arising from RSO membrane vesicles (100 μg of protein/ml), ISO membrane vesicles (100 μg of protein/ml), or proteoliposomes (30 μg of protein/ml) incubated in the presence of the sugar fluorescent analog D^2G at a final concentration of 10 μM were obtained at 100 mM KPi buffer (pH 7.0) containing 100 mM KCl.

2.8. Measurements of the Na^+-activation constant and melibiose inhibitory constant using the D^2G fluorescence assay

Experiments were carried out either on R149C or Cys-less RSO or ISO membranes vesicles (100 μg of protein/ml) in nominally Na^+-free, 100 mM KPi buffer (pH 7.0). Variations of the D^2G FRET signal intensity at 460 nm (bandwidth, 5 nm) upon excitation at 290 nm (bandwidth, 5 nm) were recorded as a function of time as Na^+ or melibiose was added stepwise as described by Guan et al. [32].

All samples were initially incubated in Na^+-free buffer containing D^2G at 10 μM, and the dependence of the intensity of the D^2G FRET signal on Na^+ concentration was analyzed following stepwise addition of NaCl to the medium at 60-s interval. The increase of the fluorescence intensity relative to the signal recorded in Na^+-free buffer was plotted as a function of cation concentration present in solution, corrected for the dilution effect and expressed as % of the maximal increase in fluorescence signal ion effect. $K_{0.5}$ Na^+ was determined by fitting the data with a hyperbolic equation.

To obtain the $K_{0.5}$ for melibiose displacement of bound D^2G, the samples were initially incubated in a medium containing 20 mM NaCl and 10 μM D^2G. Next, stepwise addition of melibiose (every 60 s) was undertaken to measure the extent of D^2G fluorescent signal extinction resulting from the displacement of bound D^2G by the competing melibiose sugar. $K_{0.5}$ for melibiose was calculated by fitting the data expressed as % of the maximal initial D^2G intensity with a hyperbolic equation.

3. Results

Like in previous works, R149C was constructed using the Cys-less MelB as a genetic background [20]. Therefore, in the following the R149C behavior will be compared to Cys-less, which displays properties very similar to those of WT [24]. A previous study of R149C in cells and RSO membrane vesicles showed that this mutant lacks binding and transport activity [20]. With the data at hand, it could not be decided whether R149C inactivation results from an overall alteration of the transporter structure or from a defect restricted to a given step of the transport cycle. To find out which is the defect introduced by the mutation, we first analyzed whether the mutant can bind the substrates once reconstituted into the liposomes, where the MelB orientation is inside-out (see Ref. [10] and below). To this end, we used infrared and fluorescence spectroscopy.

3.1. R149C reconstituted in proteoliposomes binds substrates: infrared difference spectra

Prior to analysis of the substrate-induced conformational changes by infrared difference spectroscopy, we looked for any structural change of the mutants carrying a Cys, Lys or Gln in place of Arg149. This information can be extracted from the second derivative of the IR absorbance spectra in the structure-sensitive amide I and II regions measured in the absence of substrates (Supplementary Fig. S2). It is observed that Cys-less, R149C and R149K show almost identical spectra, and thus presumably a highly conserved structure, while R149Q shows few small band-shifts in comparison to Cys-less, suggesting some minor local structural alterations. These results discard global conformational alteration, like protein denaturation or aggregation, as a possible origin of the absence of transport activity for R149C.

It has been previously shown that measuring the substrate-induced IR_{diff} spectra on purified WT or Cys-less transporters reconstituted in liposomes provides a means to assess whether or not the ionic and sugar substrates bind to the transporters and trigger conformational changes [21,33,34]. We first compare the Na^+-induced IR_{diff} spectra ($Na^+ \cdot$MelB versus $H^+ \cdot$MelB) recorded from R149C or from Cys-less after addition of 10 mM NaCl, a sodium concentration shown to be near saturating for both permeases (see below). Fig. 1A shows that a very significant

signal is recorded from R149C. To make the quantitative comparison between a mutant and Cys-less as unbiased as possible, a linear regression analysis encompassing the structure-sensitive 1710–1500 cm^{-1} region from the difference spectra was applied [19]. This global analysis provides two outputs (Fig. 1C). First, the spectral similarity of a mutant relative to the Cys-less quantifies the percentage of spectral features in common with the control Cys-less. A high spectral similarity for a mutant is expected to correlate with structural changes in response to the substrate highly similar to those of the Cys-less. Second, the relative intensity quantifies the amount of spectral features in common with the Cys-less. A relative intensity lower than 100% for any given mutant implies either a reduced affinity for the added substrate or smaller structural changes in response to substrate binding than for the Cys-less. Application of this spectral correlation analysis shows that R149C has an intensity of ~90% and a spectral similarity of ~44% with respect to Cys-less (Fig. 1C, left side). At this stage, it is important to recall that no measurable signal is detected in MelB mutants with impaired capacity to bind sodium [19]. These data prove that Na^+ not only binds to the R149C mutant, but also that binding of the Na^+ ions induces conformational changes comparable to those occurring in the Cys-less. One can however note that the R149C and Cys-less spectra display a few spectral differences, especially in the intensity of some peaks located in the amide I region (see Fig. 1A and S3A). Namely, the peaks at 1657 cm^{-1} and 1663 cm^{-1}, proposed to arise from transmembrane α-helices [18] are absent and strongly reduced in intensity in R149C. In contrast, the peak at 1651 cm^{-1} arising from another α-helix structure [18], is enhanced in R149C and slightly shifted. Peaks assigned to environment changes in deprotonated Asp side chains, at around 1404 cm^{-1}, appear to be also altered in the mutant. Therefore, Na^+ binding to R149C gives rise to slightly modified conformational changes as compared to those of the active Cys-less permease.

The R149C spectral response to addition of 50 mM melibiose in the presence of Na^+ was next investigated (Fig. 1B). The spectrum exhibits an overall shape comparable to that of Cys-less (about 84% similarity; Fig. 1C, right side) and 81% intensity, with the latter suggesting that R149C has slightly lower affinity for the sugar than Cys-less. This interpretation is coherent with equivalent experiments done with 10 mM melibiose giving rise to a difference spectrum of about 55% intensity of the Cys-less. But more importantly, the above observations imply that, like sodium, melibiose can bind to the non-transporting R149C mutant. There are some variations in the amide I region, including the decrease of the peak at 1668–1669 cm^{-1}, that may correspond to α-helix or turn structure [18] and the decreased intensity of the negative peak at 1645 cm^{-1}, assigned to β-sheet, 3_{10} helices or open loops [18]. These and other changes are better resolved after band narrowing by maximum entropy deconvolution (Supplementary Fig. S3B).

To evaluate the effect of the charge of Arg149, we analyzed two additional mutants, namely R149K and R149Q. A previous report showed that both remain functional, although with decreased transport efficiency [20]. The Na^+-induced IR_{diff} spectra of these 2 mutants are comparable to that of Cys-less, with a similarity of 57% for R149K and 69% for R149Q (Supplementary Fig. S4A–C), indicating that both mutants bind Na^+. A more thoughtful comparison shows that Na^+-induced IR_{diff} spectra are very similar between R149K and R149Q (>90% similarity), and slightly more similar to Cys-less than to R149C (Supplementary Fig. S4D). It suggests that mutation of Arg149 to Lys or Gln is more conservative than its mutation to Cys from the point of view of Na^+ binding. The sugar-induced difference spectra in the presence of Na^+ recorded from R149K and R149Q show also a high similarity to Cys-less (between 70 and 80%, Supplementary Fig. S5C), confirming these two mutants retain native-like melibiose-induced conformational changes. However, the spectral intensity is roughly half of R149C, suggesting that the affinity for melibiose might be further reduced in both R149K and R149Q. In agreement, a spectral correlation matrix suggests that for melibiose binding, mutation of Arg149 to Cys is more conservative than its mutation to Lys or Gln (Supplementary Fig. S5D).

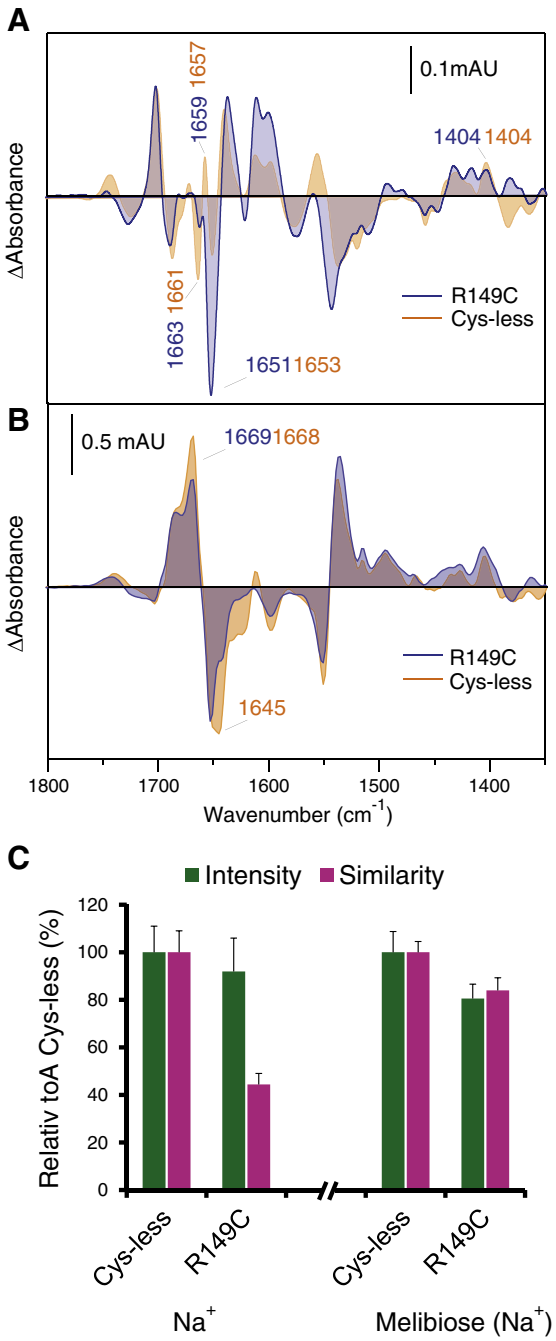

Fig. 1. Substrate-induced conformational changes. Substrate-induced IR_{diff} spectra of MelB Cys-less (orange) and R149C (blue) at 25 °C and pH 6.6 (20 mM MES and 100 mM KCl), normalized to the amount of probed protein (see Supplementary Fig. S2). (A) 10 mM Na^+-induced IR_{diff} spectra. (B) 50 mM melibiose-induced IR_{diff} spectra in the presence of 10 mM Na^+. (C) Spectral similarity and intensity of the substrate-induced IR_{diff} spectra. The error bar corresponds to one standard error of the mean of three independent spectra.

3.2. Intrinsic fluorescence spectra and Förster resonance energy transfer in R149C

To give more strength to the conclusion drawn by IR_{diff} spectroscopy that purified R149C in proteoliposomes does retain the capacity to bind Na^+ and melibiose and triggers associated conformational changes, we undertook complementary studies with the same proteoliposomes. We used intrinsic fluorescence of Trp and Förster resonance energy transfer (FRET) spectroscopy, since these techniques were previously shown to bring significant information on these MelB properties [22,23,35]. In the

absence of Na^+, incubation of R149C with melibiose (10 mM) leads to an intrinsic fluorescence increase (Fig. 2A). This signal is further enhanced after Na^+ addition because of the induced affinity increase for melibiose upon Na^+ binding [22]. These substrate-induced changes are about half the intensity observed in Cys-less, in concordance with the reduced melibiose affinity of R149C deduced from IR_{diff} experiments. The results not only confirm that R149C retains melibiose and Na^+ binding capacity, but also indicate that the reciprocal activation of the binding of one substrate by the other is maintained in R149C proteoliposomes, even if it looks somewhat altered, in keeping with the IR_{diff} spectroscopy results.

Substrate binding to proteoliposomes was also assessed using FRET from Trp residues to the fluorescent sugar analog 2′-(N-dansyl)-aminoethyl-1-thio-D-galactopyranoside (D^2G) [23]. Fig. 2 shows that, as D^2G was added, the Trp fluorescence signal (band around 330 nm) decreased in part because of FRET from Trp side chains to D^2G bound to the sugar-binding site [23]. Concomitantly, the fluorescence emission from the protein-bound fluorescent sugar appears with a maximum at 460 nm. Subsequent addition of Na^+ enhances the affinity for the sugar analog and increases its bound fraction, leading to a further increase of FRET [23]. It is worth noting that the variations of the Trp and D^2G fluorescence are linked in a complex manner. Hence, Trp fluorescence changes do not exactly mirror the variations of the D^2G fluorescence changes as would be expected for an ideal FRET process. There are at least two reasons for this behavior. First, substrate binding affects the intensity of Trp intrinsic fluorescence (see above), an effect that in some cases almost compensates for the Trp fluorescence decrease due to FRET with the D^2G. Second, MelB contains 8 Trp residues, and not all contribute as donors to the FRET process [36]. Therefore, a strict correspondence between the D^2G and Trp intensity variations is not anticipated. In Fig. 2B, C it is also seen that addition of excess melibiose decreases the FRET signal, indicating that the fluorescent sugar and melibiose compete for the same binding site.

The Na^+-dependent D^2G FRET fluorescence can be obtained from the difference between the FRET spectra recorded after and before addition of NaCl (Fig. 2D). It is important to note that the λ_{max} of the D^2G fluorescence bound to R149C (around 460 nm) is similar to that bound to the Cys-less MelB and different from D^2G interacting with lipids alone in liposomes (around 500 nm) or from D^2G dissolved in buffer (around 550 nm). This suggests that the probe experiences an equivalent hydrophobic environment when bound to the two permeases. Overall, these data show that the fluorescent sugar analog can bind to the R149C mutant, and that Na^+ retains the capacity to increase the affinity of the mutant for the sugar.

3.3. Orientation of the protein and accessibility of the sugar-binding sites in R149C vesicles and proteoliposomes

The observations described above strongly support the assertion that the R149C permease does bind sugars in proteoliposomes, but are in contradiction with previous conclusion drawn from studies on RSO membrane vesicles that this same mutant has impaired sugar-binding activity [20]. An attractive explanation for this contradiction is to assume that the difference in binding capacity observed in the two membrane types may be related to an opposite orientation of the MelB transporters in these membranes. In RSO vesicles, as in cells, the

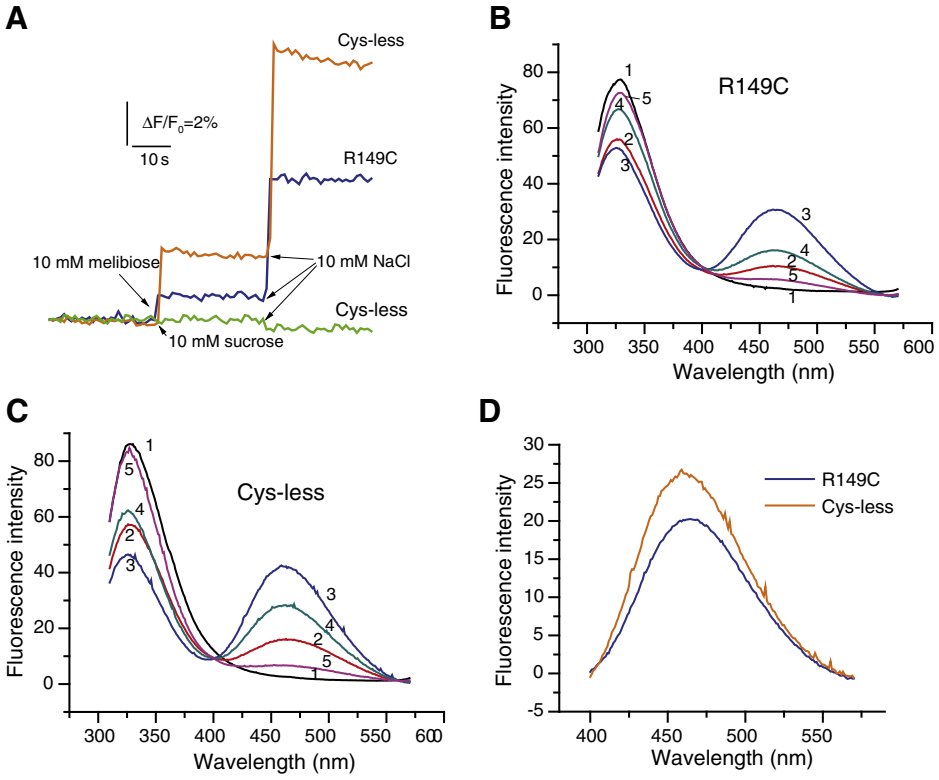

Fig. 2. Substrate-induced fluorescence changes of MelB in proteoliposomes and FRET changes. (A) Trp fluorescence changes in proteoliposomes (λ_{ex} = 290 nm, half-bandwidth = 5 nm; λ_{em} = 325 nm, half-bandwidth = 5 nm) containing purified R149C (or Cys-less) at 20 μg/ml in 100 mM KPi after the addition of sugar and Na^+ to a final concentration of 10 mM (see arrows). Sucrose addition is included as a negative control. (B) FRET signal between R149C Trp and the fluorescent sugar analog D^2G (λ_{ex} = 290 nm; half-bandwidth = 5 nm) in nominally Na^+-free 100 mM potassium phosphate and 100 mM KCl. The emission fluorescence was recorded before (trace 1) and after the consecutive additions of 15 μM D^2G (trace 2), 10 mM NaCl (trace 3), 10 mM melibiose (trace 4) and 150 mM melibiose (trace 5). Each spectrum is the mean of three scans. (C) FRET signal for Cys-less, under the same conditions and substrate additions as for R149C. (D) Na^+-induced FRET signal changes, calculated from the difference between the fluorescence spectra recorded after (trace 3 in (B) or (C)) and before addition of NaCl (trace 2 in (B) or (C)).

periplasmic side of MelB faces the outside medium; in proteoliposomes [10], as in ISO vesicles [37], MelB has an inverted orientation with the cytoplasmic side facing the outside medium. Because knowledge of the transporter orientation is critical to consider this interpretation, we felt it necessary to directly verify the orientation of the MelB permease in the RSO and ISO membrane vesicles and in the proteoliposome preparations used in the present study.

3.4. Orientation of MelB in vesicles and liposomes

Determination of MelB orientation in RSO and ISO vesicles as well as in proteoliposomes consisted in labeling two MelB mutants with strategically chosen single-Cys replacements, with the fluorescent probe tetramethylrhodamine-5-maleimide (TMRM) and comparing them to R149C. Based on a secondary structure model and current 3D MelB models [14,19,38] we produced, besides R149C, additional single-Cys mutants of MelB: I262C, with its Cys located within the putative periplasmic loops 7–8, and R139C, with its Cys located within the putative cytoplasmic loops 4–5 (Supplementary Fig. S6). To assess the location of these single-Cys in each 3 membrane preparations, the samples were pre-treated (or not) with the hydrophilic, membrane-impermeant thiol reagent, (2-(trimethylammonium)ethyl) methane thiosulfonate (MTSET) to afford protection against subsequent TMRM labeling of cysteinyl residues in contact with the extravesicular medium. Any interpretation of the results of the labeling experiments will have to take into account that TMRM is a hydrophobic SH-reagent that diffuses across the membrane under our experimental conditions [28]. Therefore, TMRM is able to label cysteines contained in proteins on the inner side of the membrane vesicles. The same protocol was then used to label the R149C mutant and the Cys-less MelB, with the latter taken as an index of selectivity of the labeling procedure.

The results of the labeling analysis illustrated in Fig. 3A correspond to measurements of signals from permeases purified after TMRM labeling and submitted to electrophoresis. As first seen in Fig. 3A, I262C and R139C vesicles are labeled by TMRM in both RSO and ISO vesicles if previous incubation with the impermeant MTSET was omitted. In addition, the data clearly show that MTSET pretreatment very efficiently protects against the labeling of I262C in RSO vesicles but not in ISO vesicles. In contrast, MTSET does not prevent TMRM labeling in R139C RSO vesicles, and totally hampers TMRM to react with this cysteine residue in ISO vesicles. Importantly, the total absence of TMRM labeling in Cys-less RSO or ISO vesicles (Fig. 3C), discards any non-specific labeling of MelB or other proteins present in the vesicles. Taken as a whole, these results reveal that the two membrane vesicle populations used in the present study are largely homogeneous and possess the expected right-side out orientation in RSO and an inside-out one in ISO vesicles.

Fig. 3A also shows that R149C TMRM labeling takes place in RSO vesicles irrespective of pre-treatment or not with MTSET. Conversely, TMRM labeling takes place in R149C ISO vesicles untreated with MTSET but is totally absent in ISO vesicles previously reacted with MTSET. These results imply that in the RSO vesicles the single cysteine of R149C faces the intravesicular medium, whereas in ISO vesicles it faces to the external medium.

The same TMRM labeling/MTSET protection procedure was used to analyze the MelB orientation of the different single-Cys mutants in proteoliposomes (Fig. 3B). It can be seen that the impermeant SH-reagent MTSET prevents the labeling of R139C, but not that of I262C. In addition, and as observed in R149C ISO vesicles, MTSET also shields R149C from being labeled by TMRM. One can therefore conclude that MelB in proteoliposomes has an inside-out orientation, i.e. the same as that observed in ISO vesicles. This conclusion agrees with previous evidence for an inside-out orientation of MelB in proteoliposomes [10].

3.5. Accessibility of the sugar-binding sites: Na^+-induced change of the FRET signal

To study the accessibility of the sugar-binding site in vesicles, we recorded the FRET signal changes of the fluorescent sugar analog D^2G induced by sodium [23], in both ISO and RSO membrane vesicles and normalized the spectra with respect to total protein content (Fig. 4A to G). No significant or at best a very weak Na^+-induced FRET signal was recorded for R149C in RSO vesicles (Fig. 4E, black line), in complete agreement with previous results [20] even though a significant presence of MelB could be confirmed using a His-Tag specific reagent. In that work, Abdel-Dayem et al. [20] not only showed lack of binding of D^2G in RSO as we show here, but also of the labeled sugar analog [^{3}H]p-nitrophenyl-α-D-galactopyranoside (NPG). Furthermore, we found no significant differences between the fluorescence signal in R149C RSO vesicles and in RSO or ISO vesicles prepared from DW2 cells that do not express MelB, which were used as controls (Supplementary Fig. S7). It is therefore evident that sugars cannot bind to R149C RSO vesicles. In contrast to these results, a clear FRET signal was observed in R149C ISO vesicles (Fig. 4E, red line), similar to that observed for proteoliposomes in Fig. 2. We also analyzed the responses of RSO and ISO vesicles from cells expressing R139C, I262C, WT, Cys-less, R149K, and R149Q MelB (Fig. 4). A final control was done by corroborating that the FRET signal indeed decreased and eventually disappeared by adding excess of melibiose.

The ratio between the Na^+-dependent FRET signals in ISO and RSO vesicles (ISO/RSO) carrying any single mutant was used as a quantitative index of the relative accessibility of D^2G to the sugar-binding site from the periplasmic or from the cytoplasmic sides in each transporter (Fig. 4H). For R139C, I262C, WT, Cys-less, and R149K permeases the ratio of ~1 indicates equal accessibility from either sides. With a ratio of ~2.5, R149Q seems to have a slightly easier access from the periplasmic side than from the cytoplasmic one. Remarkably, the ratio for R149C reaches a value of about ~26 when the signals are corrected for total protein content in vesicles. MelB quantification by a His-Tag specific reagent indicates a similar distribution in ISO and RSO Cys-less vesicles, but systematically asymmetrical for R149C. After correction for the 3–4 times lower fraction of R149C in the RSO than in the ISO vesicles, the FRET ratio is reduced to ~7, a value still notably high (Fig. 4H). As a whole, these results indicate that intracellular sugar can reach the substrate-binding site in R149C but hardly any extracellular sugar does.

To achieve a more complete characterization of the co-substrate binding properties of R149C and their comparison with those of the Cys-less, we used D^2G as a reporter of sugar binding and determined the constants of activation by Na^+ ($K_{0.5}$ [Na^+]) and of the inhibition by melibiose ($K_{0.5}$ [mel]) of the fluorescent probe binding in RSO and ISO vesicles [32] (supplementary Table S1). In Cys-less ISO and RSO vesicles, the $K_{0.5}$ [Na^+] values are nearly identical. This observation supports the common idea that the inward and outward conformations share the same binding site. Therefore, any mutation affecting the binding site is expected to affect similarly to the inward and outward conformations. In addition, a slightly higher value was found in R149C ISO vesicles. This indicates that the Na^+ affinity and the Na^+-sugar coupling are barely modified in R149C. The insignificant D^2G FRET signal R149C RSO vesicles (Fig. 4E) precluded the determination of the constants in these membranes.

Regarding the inhibition of D^2G binding by melibiose ($K_{0.5}$ [mel]), the values of 3.79 and 2.66 mM in Cys-less ISO and RSO vesicles, respectively (Table S1) suggest a slightly better binding affinity for melibiose originating from the outer medium than for melibiose originating from the cytoplasmic medium. Interestingly, the $K_{0.5}$ [mel] values found in Cys-less (3.79 mM) and R149C (5.01 mM) ISO vesicles have the same order of magnitude, and suggest that the mutation of Arg into Cys causes a limited reduction of affinity for the sugar. As a whole, these results strongly suggest that the co-substrate binding process of the mutated permease is only moderately affected by the mutation, in agreement

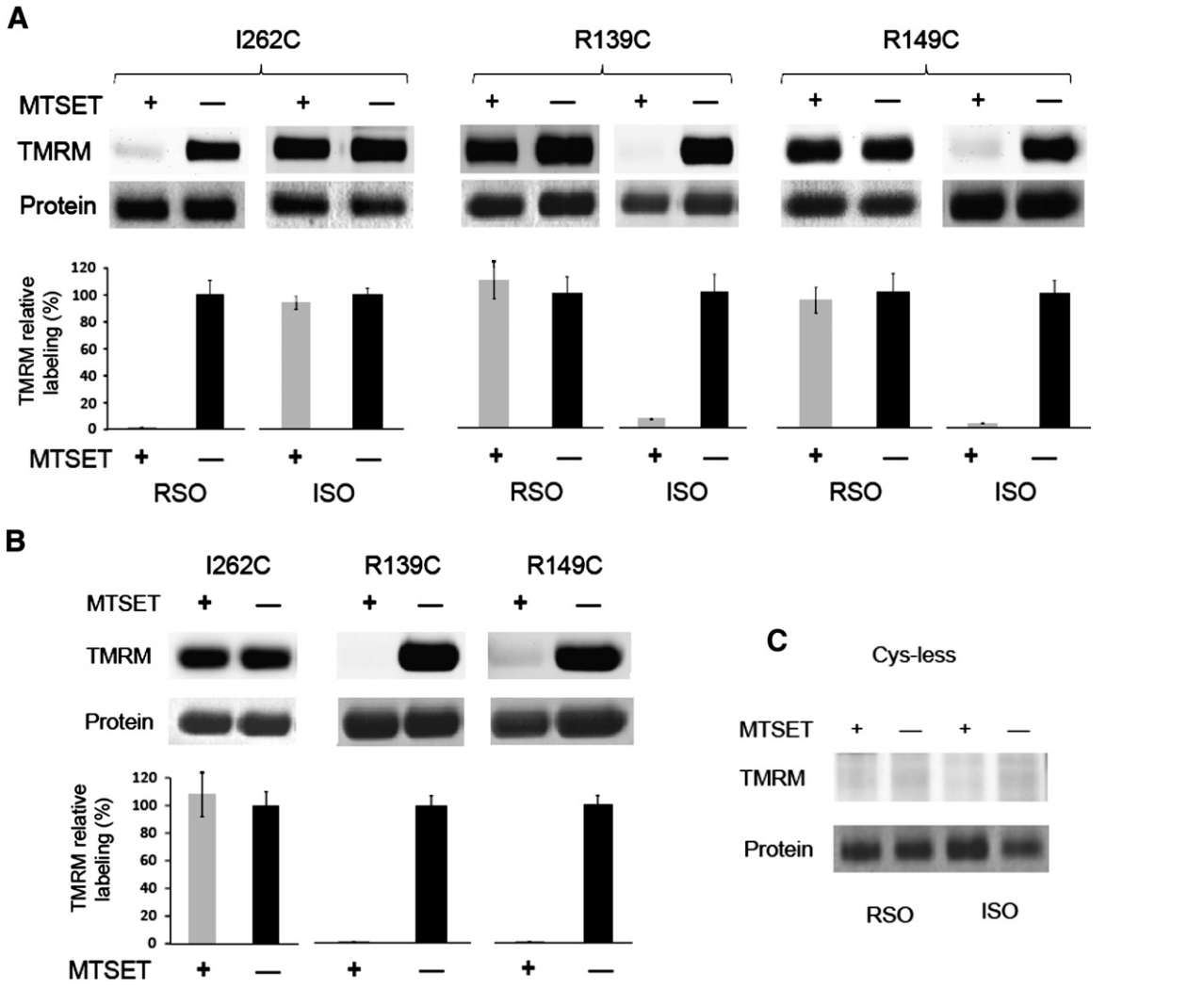

Fig. 3. Orientation of R149C in vesicles and proteoliposomes. (A) RSO or ISO membrane vesicles at 30 μg/ml of protein containing I262C, R139C or R149C single cysteine mutants were reacted with 40 μM TMRM directly, or after pretreatment with 0.1 mM MTSET. MelB was purified from the solubilized vesicles and subjected to SDS-PAGE. The Coomassie-stained bands report the amount of the loaded MelB protein, and the TMRM reacted with MelB was imaged on the gel using the TMRM intrinsic fluorescence as described in Materials and methods. Histograms represent the ratio between the intensity of TMRM and protein bands area, expressed relative to the vesicles without treatment with MTSET. Each value is the mean of three independent experiments (±S.E.). (B) Orientation of I262C, R139C or R149C in proteoliposomes. The experiments were performed as in (A). (C) TMRM labeling of MelB Cys-less mutant in ISO and RSO vesicles, following the same protocol as in (A).

with IR_{diff} and fluorescence data in proteoliposomes. In contrast, the mutation appears to induce a major defect in the reorientation mechanism required for MelB to adopt an outward-facing conformation.

4. Discussion

The FTIR and fluorescence results presented in this work show: (i) that R149C, R149K, and R149Q bind Na^+ and melibiose in proteoliposomes, where the transporter has an inverted orientation with respect to that in the cell i.e., with the cytoplasmic side oriented to the exterior medium; (ii) that the conformational changes induced by Na^+ or sugar binding to the R149C mutant are comparable to the Cys-less transporter albeit with a few significant differences in α-helical structures, indicating that the mutation affects the interaction of Na^+ and the sugar with the transporter; (iii) that Na^+ and the fluorescent sugar analog D^2G, as well as melibiose are capable of accessing the R149C substrate-binding sites in inside-out membrane vesicles but not in the right-side-out vesicles. In contrast, the substrates can access the substrate-binding site in R149K and R149Q either in ISO membrane vesicles or in RSO membrane vesicles.

Previous studies in cells and RSO membrane vesicles led to the suggestion that the inability of transport by the R149C mutant was due to the fact that the permease no longer binds sugars [20]. However, our results lead clearly to a new interpretation: this mutant is able to bind substrates, but the defect introduced by the mutation consists in that R149C remains largely in an inward-facing conformation and is not capable of reorienting its binding sites to the periplasmic side. This defect explains the absence of transport in R149C, even if it is capable of binding the substrates in ISO vesicles.

According to current hypothesis on the transport mechanism by the alternate access model [6,8,39–43], a critical feature of substrate transport is the equilibrium established between the outward- and the inward-facing orientations, allowing for an efficient transport turnover (Supplementary Fig. S1). Thus, the substrate-binding sites of the empty transporter are assumed to be alternatively accessible from both sides of the membrane according to an equilibrium established between both conformations, with a free energy barrier for this conformational change in the range of the thermal energy. For MelB, this is substantiated by the similar affinity (Table S1) and accessibility (Fig. 4) of the substrates to the substrate-binding sites from both sides of the vesicles, even if the frequency of opening to the periplasmic space might be much lower than opening to the cytoplasmic space [44]. Under normal conditions, the binding of the substrates from the periplasmic side is followed by the reorientation of the

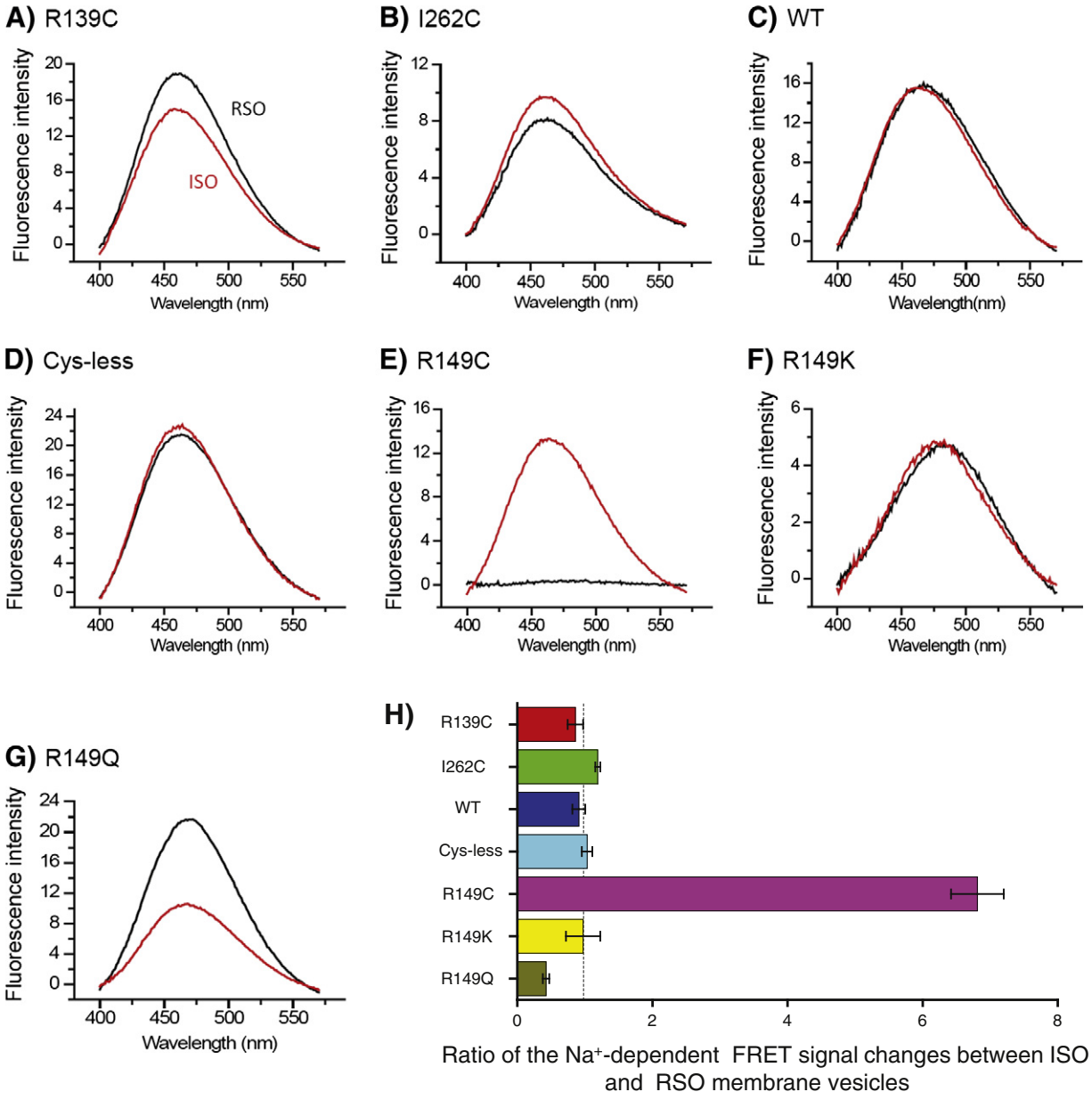

Fig. 4. Na^+-dependent variation of the FRET signal recorded from ISO and RSO membrane vesicles. ISO (red trace) or RSO membrane vesicles (black trace) were incubated with the sugar analog D^2G (10 μM) and excited at 290 nm (half-bandwidth = 5 nm). The FRET signal from Trp residues to D^2G recorded before the addition of Na^+ was subtracted from the FRET signal recorded after the addition of Na^+ (20 mM final concentration). Each Na^+-dependent variation of the FRET signal presented in (A)–(G) is the average of at least three independent experiments and was corrected for the amount of total protein. (H) Histogram showing the ratio of the Na^+-dependent FRET signal changes integrated between 400 and 570 nm, between ISO and RSO membrane vesicles. The FRET signal of R149C vesicles was corrected for differences in the MelB content measured in the two types of membrane vesicles. Values are the mean of three independent experiments (±S.E.).

outward-facing to the inward-facing conformation [6,42]. The binding process itself might also contribute to speed up the reorientation process by decreasing its free energy barrier, as it occurs in enzymatic reactions. On molecular terms, this reorientation and change in accessibility would take place by means of the so-called rocking bundle mechanism, in which some transmembrane helices or part of helices tilt as rigid bodies, in concerted movements involving also conformational changes in the helical ends and loops [7,45]. Changes of helical tilting of MelB upon substrate binding have been described by using polarized IR_{diff} spectroscopy [9], giving support to this notion. The results presented in this paper demonstrate that Arg149 is critically involved in the switching mechanism of MelB between outward and inward conformations.

The positive charge at position 149 does not seem to be an absolute requirement for the reorientation mechanism, in keeping with previous suggestions [20]. Our data demonstrate that, although R149Q shows easier access from the extracellular side, it is accessible to the fluorescent sugar analog from both sides (Fig. 4). On the other hand, R149K shows the same accessibility as Cys-less from both sides. The IR_{diff} spectra for these two mutants are altered in shape and are reduced in intensity, especially for sugar binding (Supplementary Figs. S4 and S5), indicating that both mutations affect substrate binding and reduce the affinity for melibiose. These results are in agreement with a previous work reporting that these mutants retain 25–30% of transport efficiency [20]: there is a correspondence between the accessibility to the substrate-binding site from both sides, and the transport capacity. In addition, it seems likely that the reorientation of the WT (or the Cys-less) carrier requires at least a polar residue at position 149, and that the positive charge of Arg149 would provide the optimal arrangement and interactions for an effective change of orientation and efficient transport.

In the absence of an atomic 3D structure for MelB, it is challenging to presume how Arg149 performs its role. It could be hypothesized that Arg149, most probably located in the inner (cytoplasmic) half of TM5, could interact with a side chain of TM4 (Fig. 5A). It could form a hydrogen bond with Tyr120 or a salt bridge with Asp124, both located favorably in TM4 in a recent MelB model [38]. One or both of these interactions could be crucial for stabilizing the helix tilt changes, and without them the energy barrier for the reorientation of the binding sites might largely increase, explaining the effect of R149C mutation. In this regard, it has been proposed that TM4 in MelB could behave as a hinge for the required helical movements during transport [20,35]. In TM4, Gly117 has also been implicated in the reorientation mechanism [46]. In this case, the mutant was proposed to be in an initial outward-facing conformation, contrary to R149C. It could be envisaged that the contiguous TM4 (where Gly117 is located) and TM5 (containing Arg149) could undergo coordinated movements during transport by a mechanism in which both side chains are critical components (Fig. 5B). Comparison with the *E. coli* lactose permease (LacY), another member of the major facilitator superfamily, can help to set up a reasonable hypothesis. In LacY, Arg144, located in TM5, is irreplaceable for active lactose transport by establishing alternating salt bridges with Glu126 and Glu269 side chains during transport [47]. It is remarkable that the two available predictions about the MelB structure propose a similar location of Arg149 compared to Arg144 of LacY in TM5 and of Asp124 compared to Glu126 of LacY in TM4 [38] (see Supplementary Fig. S8). In addition, it is worth noting that the putative TM5 of MelB, like the corresponding region of LacY, contains two Gly side chains that may facilitate the reorientation movements.

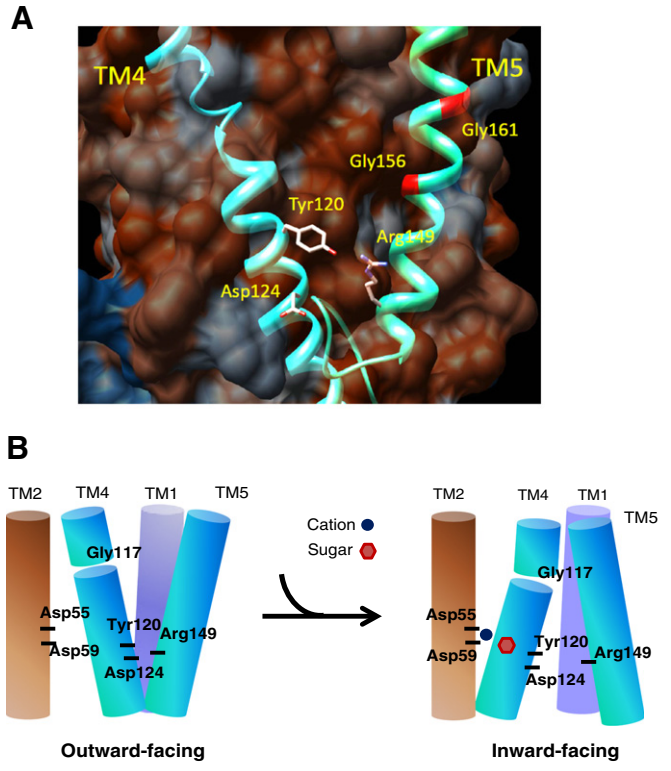

Fig. 5. (A) Model of helices TM4 and TM5 of MelB. The location of Gly residues in TM5 is marked in red color. The MelB model was obtained from Yousef and Guan [38]. (B) Cartoon showing a hypothetical mechanism for the reorientation of the substrate-binding site between the outward- and inward-facing conformations. Arg149 would be essential to maintain equilibrium between both orientations for the empty MelB, thanks to its interaction with Asp124 and/or Tyr120. Substrate binding would displace the equilibrium towards the inward-facing conformation, allowing their release to the cytoplasm. Mutation of Arg149 to Cys will block the transporter in the inward facing conformation. Gly117 would have a decisive role in the movement of helix 4 [46]. Asp55 and Asp59 in helix 2 are ligands to Na^+, while Asp19 in helix 1 (not shown) is a ligand for the sugar [19].

Importantly, a mutation also in TM5 of LacY (C154G) has been described to stabilize the transporter in one conformation that allows sugar binding from both sides, but cannot undergo the conformational changes on the periplasmic side required for translocation [8,48,49]. It is therefore tempting to speculate that key side chains in TM5 of MelB participate in interactions important for the reorientation mechanism and that Arg149 could perform a similar role as Arg144 of LacY. In this scenario, Arg149 could be ion paired with Asp124 and/or hydrogen bonded to Tyr120, both located in TM4, in addition to directly participating in sugar binding. These interactions could be essential for the reorientation mechanism or, at least, for the opening of the periplasmic side. The observation that in all the studied Arg149 mutants both Na^+ and melibiose-induced structural changes are in some way altered favors an interaction of Arg149 with Asp124, a residue found to be essential in coupling the Na^+ and melibiose-binding site [19]. To give more strength to this hypothesis, it is worth to consider that, in the cases where inward- and outward-facing structures have been obtained, like in the LeuT transporter, several ionic interactions form and break upon going from outward- to inward-facing or vice-versa [50]. Arg149 in MelB could be one of the side chains participating directly in ionic interactions in a similar fashion as Arg5 or Arg30 in LeuT [50].

Acknowledgements

We would like to thank H. Ronald Kaback for insightful discussions and critical reading of the manuscript, and Elodia Serrano and Neus Ontiveros for skillful technical assistance. This work was supported by the UAB Postdoctoral Fellowship 40607 and the Marie Curie Reintegration Grant PIRG03-6A-2008-231063 (to V.L.-F.), the Ministerio de Ciencia e Innovación grant BFU2009-08758/BMC and in part by a grant from the Commissariat à l'Energie Atomique (CEA-Saclay).

Appendix A. Supplementary data

Supplementary data to this article can be found online at http://dx.doi.org/10.1016/j.bbamem.2013.03.003.

References

[1] U. Gether, P.H. Andersen, O.M. Larsson, A. Schousboe, Neurotransmitter transporters: molecular function of important drug targets, Trends Pharmacol. Sci. 27 (2006) 375–383.
[2] E. Padan, The enlightening encounter between structure and function in the NhaA Na^+–H^+ antiporter, Trends Biochem. Sci. 33 (2008) 435–443.
[3] B. Poolman, J. Knol, C. van der Does, P.J. Henderson, W.J. Liang, G. Leblanc, T. Pourcher, I. Mus-Veteau, Cation and sugar selectivity determinants in a novel family of transport proteins, Mol. Microbiol. 19 (1996) 911–922.
[4] T. Pourcher, M. Bassilana, H.K. Sarkar, H.R. Kaback, G. Leblanc, The melibiose/Na^+ symporter of *Escherichia coli*: kinetic and molecular properties, Philos. Trans. R. Soc. Lond. B Biol. Sci. 326 (1990) 411–423.
[5] T. Pourcher, S. Leclercq, G. Brandolin, G. Leblanc, Melibiose permease of *Escherichia coli*: large scale purification and evidence that H^+, Na^+, and Li^+ sugar symport is catalyzed by a single polypeptide, Biochemistry 34 (1995) 4412–4420.
[6] H. Krishnamurthy, C.L. Piscitelli, E. Gouaux, Unlocking the molecular secrets of sodium-coupled transporters, Nature 459 (2009) 347–355.
[7] L.R. Forrest, R. Kramer, C. Ziegler, The structural basis of secondary active transport mechanisms, Biochim. Biophys. Acta 1807 (2011) 167–188.
[8] H.R. Kaback, I. Smirnova, V. Kasho, Y. Nie, Y. Zhou, The alternating access transport mechanism in LacY, J. Membr. Biol. 239 (2011) 85–93.
[9] V.A. Lórenz-Fonfría, M. Granell, X. León, G. Leblanc, E. Padrós, In-plane and out-of-plane infrared difference spectroscopy unravels tilting of helices and structural changes in a membrane protein upon substrate binding, J. Am. Chem. Soc. 131 (2009) 15094–15095.
[10] K. Meyer-Lipp, N. Sery, C. Ganea, C. Basquin, K. Fendler, G. Leblanc, The inner interhelix loop 4–5 of the melibiose permease from *Escherichia coli* takes part in conformational changes after sugar binding, J. Biol. Chem. 281 (2006) 25882–25892.
[11] C. Ganea, K. Fendler, Bacterial transporters: charge translocation and mechanism, Biochim. Biophys. Acta 1787 (2009) 706–713.
[12] I. Hacksell, J.L. Rigaud, P. Purhonen, T. Pourcher, H. Hebert, G. Leblanc, Projection structure at 8 Å resolution of the melibiose permease, an Na–sugar co-transporter from *Escherichia coli*, EMBO J. 21 (2002) 3569–3574.
[13] M.C. Botfield, K. Naguchi, T. Tsuchiya, T.H. Wilson, Membrane topology of the melibiose carrier of *Escherichia coli*, J. Biol. Chem. 267 (1992) 1818–1822.

[14] T. Pourcher, E. Bibi, H.R. Kaback, G. Leblanc, Membrane topology of the melibiose permease of *Escherichia coli* studied by melB–phoA fusion analysis, Biochemistry 35 (1996) 4161–4168.
[15] A. Yamashita, S.K. Singh, T. Kawate, Y. Jin, E. Gouaux, Crystal structure of a bacterial homologue of Na^+/Cl^- dependent neurotransmitter transporters, Nature 437 (2005) 215–223.
[16] S. Faham, A. Watanabe, G.M. Besserer, D. Cascio, A. Specht, B.A. Hirayama, E.M. Wright, J. Abramson, The crystal structure of a sodium galactose transporter reveals mechanistic insights into Na^+/sugar symport, Science 321 (2008) 810–814.
[17] A. Watanabe, S. Choe, V. Chaptal, J.M. Rosenberg, E.M. Wright, M. Grabe, J. Abramson, The mechanism of sodium and substrate release from the binding pocket of vSGLT, Nature 468 (2010) 988–991.
[18] X. León, R. Lemonnier, G. Leblanc, E. Padrós, Changes in secondary structures and acidic side chains of melibiose permease upon cosubstrates binding, Biophys. J. 91 (2006) 4440–4449.
[19] M. Granell, X. León, G. Leblanc, E. Padrós, V.A. Lórenz-Fonfría, Structural insights into the activation mechanism of melibiose permease by sodium binding, Proc. Natl. Acad. Sci. U. S. A. 107 (2010) 22078–22083.
[20] M. Abdel-Dayem, C. Basquin, T. Pourcher, E. Cordat, G. Leblanc, Cytoplasmic loop connecting helices IV and V of the melibiose permease from *Escherichia coli* is involved in the process of Na^+-coupled sugar translocation, J. Biol. Chem. 278 (2003) 1518–1524.
[21] X. León, V.A. Lórenz-Fonfría, R. Lemonnier, G. Leblanc, E. Padrós, Substrate-induced conformational changes of melibiose permease from *Escherichia coli* studied by infrared difference spectroscopy, Biochemistry 44 (2005) 3506–3514.
[22] I. Mus-Veteau, T. Pourcher, G. Leblanc, Melibiose permease of *Escherichia coli*: substrate-induced conformational changes monitored by tryptophan fluorescence spectroscopy, Biochemistry 34 (1995) 6775–6783.
[23] C. Maehrel, E. Cordat, I. Mus-Veteau, G. Leblanc, Structural studies of the melibiose permease of *Escherichia coli* by fluorescence resonance energy transfer. I. Evidence for ion-induced conformational change, J. Biol. Chem. 273 (1998) 33192–33197.
[24] A.C. Weissborn, M.C. Botfield, M. Kuroda, T. Tsuchiya, T.H. Wilson, The construction of a cysteine-less melibiose carrier from *E. coli*, Biochim. Biophys. Acta 1329 (1997) 237–244.
[25] M.C. Botfield, T.H. Wilson, Mutations that simultaneously alter both sugar and cation specificity in the melibiose carrier of *Escherichia coli*, J. Biol. Chem. 263 (1988) 12909–12915.
[26] O.H. Lowry, N.J. Rosebrough, A.L. Farr, R.J. Randall, Protein measurement with the Folin phenol reagent, J. Biol. Chem. 193 (1951) 265–275.
[27] H.R. Kaback, Bacterial membranes, Methods Enzymol. XXII (1971) 99–120.
[28] Y. Nie, N. Ermolova, H.R. Kaback, Site-directed alkylation of LacY: effect of the proton electrochemical gradient, J. Mol. Biol. 374 (2007) 356–364.
[29] Y. Nie, F.E. Sabetfard, H.R. Kaback, The Cys154 → Gly mutation in LacY causes constitutive opening of the hydrophilic periplasmic pathway, J. Mol. Biol. 379 (2008) 695–703.
[30] L. Guan, H.R. Kaback, Site-directed alkylation of cysteine to test solvent accessibility of membrane proteins, Nat. Protoc. 2 (2007) 2012–2017.
[31] V.A. Lórenz-Fonfría, E. Padrós, Maximum entropy deconvolution of infrared spectra: use of a novel entropy expression without sign restriction, Appl. Spectrosc. 59 (2005) 474–486.
[32] L. Guan, S. Nurva, S.P. Ankeshwarapu, Mechanism of melibiose/cation symport of the melibiose permease of *Salmonella* typhimurium, J. Biol. Chem. 286 (2011) 6367–6374.
[33] X. León, G. Leblanc, E. Padrós, Alteration of sugar-induced conformational changes of the melibiose permease by mutating Arg141 in loop 4–5, Biophys. J. 96 (2009) 4877–4886.
[34] V. Lórenz-Fonfría, X. León, E. Padrós, Studying substrate binding to reconstituted secondary transporters by attenuated total reflection infrared difference spectroscopy, Methods Mol. Biol. 914 (2012) 107–126.
[35] E. Cordat, G. Leblanc, I. Mus-Veteau, Evidence for a role of helix IV in connecting cation- and sugar-binding sites of *Escherichia coli* melibiose permease, Biochemistry 39 (2000) 4493–4499.
[36] E. Cordat, I. Mus-Veteau, G. Leblanc, Structural studies of the melibiose permease of *Escherichia coli* by fluorescence resonance energy transfer. II. Identification of the tryptophan residues acting as energy donors, J. Biol. Chem. 273 (1998) 33198–33202.
[37] C. Gwizdek, G. Leblanc, M. Bassilana, Proteolytic mapping and substrate protection of the *Escherichia coli* melibiose permease, Biochemistry 36 (1997) 8522–8529.
[38] M.S. Yousef, L. Guan, A 3D structure model of the melibiose permease of *Escherichia coli* represents a distinctive fold for Na^+ symporters, Proc. Natl. Acad. Sci. U. S. A. 106 (2009) 15291–15296.
[39] O. Jardetsky, Simple allosteric model for membrane pumps, Nature 211 (1966) 969–970.
[40] T. Shimamura, S. Weyand, O. Beckstein, N.G. Rutherford, J.M. Hadden, D. Sharples, M.S. Sansom, S. Iwata, P.J. Henderson, A.D. Cameron, Molecular basis of alternating access membrane transport by the sodium–hydantoin transporter Mhp1, Science 328 (2010) 470–473.
[41] S. Radestock, L.R. Forrest, The alternating-access mechanism of MFS transporters arises from inverted-topology repeats, J. Mol. Biol. 407 (2011) 698–715.
[42] L.R. Forrest, G. Rudnick, The rocking bundle: a mechanism for ion-coupled solute flux by symmetrical transporters, Physiology (Bethesda) 24 (2009) 377–386.
[43] Y. Zhou, L. Guan, J.A. Freites, H.R. Kaback, Opening and closing of the periplasmic gate in lactose permease, Proc. Natl. Acad. Sci. U. S. A. 105 (2008) 3774–3778.
[44] I. Smirnova, V. Kasho, J. Sugihara, H.R. Kaback, Opening the periplasmic cavity in lactose permease is the limiting step for sugar binding, Proc. Natl. Acad. Sci. U. S. A. 108 (2011) 15147–15151.
[45] C.J. Law, P.C. Maloney, D.N. Wang, Ins and outs of major facilitator superfamily antiporters, Annu. Rev. Microbiol. 62 (2008) 289–305.
[46] C. Ganea, K. Meyer-Lipp, R. Lemonnier, A. Krah, G. Leblanc, K. Fendler, G117C MelB, a mutant melibiose permease with a changed conformational equilibrium, Biochim. Biophys. Acta 1808 (2011) 2508–2516.
[47] O. Mirza, L. Guan, G. Verner, S. Iwata, H.R. Kaback, Structural evidence for induced fit and a mechanism for sugar/H^+ symport in LacY, EMBO J. 25 (2006) 1177–1183.
[48] I.N. Smirnova, H.R. Kaback, A mutation in the lactose permease of *Escherichia coli* that decreases conformational flexibility and increases protein stability, Biochemistry 42 (2003) 3025–3031.
[49] L. Guan, O. Mirza, G. Verner, S. Iwata, H.R. Kaback, Structural determination of wild-type lactose permease, Proc. Natl. Acad. Sci. U. S. A. 104 (2007) 15294–15298.
[50] H. Krishnamurthy, E. Gouaux, X-Ray structures of LeuT in substrate-free outward-open and apo inward-open states, Nature 481 (2012) 469–474.